# Measured 21.5 GHz Indoor Channels With User-Held Handset Antenna Array

Hejselbæk, Johannes; Nielsen, Jesper Ødum; Fan, Wei; Pedersen, Gert F.

*Published in:*
I E E E Transactions on Antennas and Propagation

*DOI (link to publication from Publisher):*
10.1109/TAP.2017.2742556

*Publication date:*
2017

*Document Version*
Accepted author manuscript, peer reviewed version

# Measured 21.5 GHz Indoor Channels With User-Held Handset Antenna Array

Johannes Hejselbæk, *Student Member, IEEE,* Jesper Ødum Nielsen, Wei Fan, *Member, IEEE,* and Gert Frølund Pedersen, *Senior Member, IEEE*

***Abstract*—For mobile systems involving hand held devices, the influence of the user on system performance has to be considered. Extensive studies below 6 GHz have demonstrated large effects on system performance. However, the impact of user influence at potential higher frequency bands for upcoming 5G mobile networks is still to be investigated. This work investigates how the user affects the performance of a 5G handset mock-up. The user impact is studied by channel sounding in an indoor scenario, with and without the presence of different users. The mock-up handset has a uniform linear array of receive (Rx) antennas operated at 21.5 GHz. A dual-polarized horn antenna with a wide beamwidth is used as transmit (Tx) antenna and a fast channel sounder is used, allowing for recording dynamic and realistic channels. The results show that the mean influence of the user on the power varies considerably depending on the scenario, with more than 12 dB loss in some cases, while a gain of 4 dB is seen in other. An important finding is that the mean power among the seven Rx branches may be very different. Branch power ratios in the typical range of 2–10 dB were found, depending on the user and scenario.**

***Index Terms*—Radio propagation, channel sounding, user impact, 5G, mobile antenna, indoor environments, user blocking.**

## I. Introduction

THE increasing demand for mobile broadband is one of the driving factors behind the development of the fifth generation (5G) mobile communication network [1], [2]. To provide the required high data rate and capacity, there is a strong need for unused spectrum, which is scarce below 6 GHz. Due to this, multiple frequency bands in the centimetre- and millimetre-wave range above 6 GHz have been suggested [2]–[5].

Historically, frequency bands below 6 GHz have been preferred for cellular usage mainly due to generally increasing pathloss causing coverage issues at high frequency bands. However, these challenges can be overcome by applying high gain directional antennas, as explained in [6], [7]. Further, the increase in frequency and thereby shorter wavelengths makes it possible to fit more antennas in a small form-factor such as a mobile terminal [8]. This allows for directive antenna arrays which can be used for beam steering/forming [9]–[11]. Knowledge of channel characteristics is crucial for 5G system design and performance evaluation. As a result, strong efforts on channel measurements at the proposed frequencies for 5G have been made both from industry and academia.

For the unlicensed frequency band at 60 GHz, used for IEEE 802.11ad wireless local area networks (WLANs), a significant amount of channel studies are available [12]–[16]. However, 60 GHz is suitable only for short-range communications because of high path loss. Due to this, lower frequencies, which are more suitable for cellular communications, have been studied, ranging from 20 GHz to 40 GHz, see e.g. [6], [11], [17]–[26]. However, the focus of existing work has been on channel characteristics, e.g. path-loss, angle of arrival (AoA) and delay-spread (DS) in static or quasi-static environments.

The human blocking effect is a well-studied phenomenon in the 60 GHz range where it was shown that the propagation path can be attenuated by more than 20 dB due to human blocking [27], [28]. The fading characteristics of human movement in a 26 GHz point-to-point indoor static scenario have been reported in [29]. The results showed that more severe received power variation occurred in the 26 GHz band compared with the 2 GHz band. The human body can effectively block the radio path at millimetre-wave bands. This implies that the user impact is important to describe in the propagation environment. In order to investigate the influence that users have on a handset antenna performance, it is necessary to use antennas and handset designs close to what they will be in the intended application. In related work [30], [31], a linear phased array operating at 15 GHz was studied, and it was demonstrated that the blocking effect in talk mode was up to 25 dB. However, the focus was on antenna design, only investigating the completely static user impact in an anechoic chamber. User influence, together with propagation environments and antenna designs, determines how well multiple-input multiple-output (MIMO) handset terminals operate in true usage conditions. It is well-known that 5G systems at millimetre-wave bands will suffer rapid channel dynamics, due to the high Doppler shift and blockage. As a result, it is important to evaluate user influence on feasible 5G antenna designs in dynamic environments. This differs from other reported channel measurements as they in most cases have been utilizing horn antennas or virtual arrays. A horn antenna is not a feasible solution for an implementation in a user handset and these measurements cannot capture dynamic

Manuscript received October 28, 2016; revised June 30, 2017. Current version August 15, 2017. This work have been conducted under the framework of the VIRTUOSO project. The Danish National Advanced Technology Foundation supports this project together with industry partners.

J. Hejselbæk, J.Ø. Nielsen, W. Fan and G.F. Pedersen are with the Antennas, Propagation and Millimetre-wave Systems (APMS) section at the Department of Electronic Systems, TECH Faculty, Aalborg University, Denmark. Email: {joh, jni, wfa, gfp}@es.aau.dk

Color versions of one or more of the figures in this paper are available online at http://ieeexplore.ieee.org.

Digital Object Identifier xx.xxxx/TAP.xxxx.xxxxxxx

influences of users. As the main aim for 5G is to improve the data rates, it is most interesting to investigate the user impact in 'data mode', where the user holds the device in front of the body. The user influence on performance has been extensively investigated frequency bands below 6 GHz [32]–[35] and recently also at 28 GHz in anechoic conditions [36]. However, to the knowledge of the authors, a comprehensive study of user impact in a realistic dynamic environment in the millimetre-wave frequency band is missing in the literature.

The paper is structured as follows: Section II details the measurement system, measurement scenario and measurement procedure. After that the measured results are detailed in Section III and further discussed in Section IV. Finally, Section V concludes the paper.

## II. Measurement System and Setup

### A. Mock-up Handset Antenna

To investigate the user influence on the channel, a mock-up with a realistic size for a handset was designed. The mock-up handset consists of eight microstrip patch antenna elements on the top side of the handset. The antenna design was detailed in [37] and only briefly explained here. In [37], a phased array consisting of three identical sub-arrays, each with eight antenna elements, was proposed to enable 3D coverage. In this study, only the sub-array pointing towards the user is realized and used in the mock-up. The array elements can be seen on the top edge of the Printed Circuit Board (PCB) in Fig. 1, left. The individual elements are connected by a matched transmission line to an absorptive switch (Pasternack PE7173) as seen in Fig. 1, right. The center-to-center distance between the elements is around $\lambda/2$, operated at 21.5 GHz.

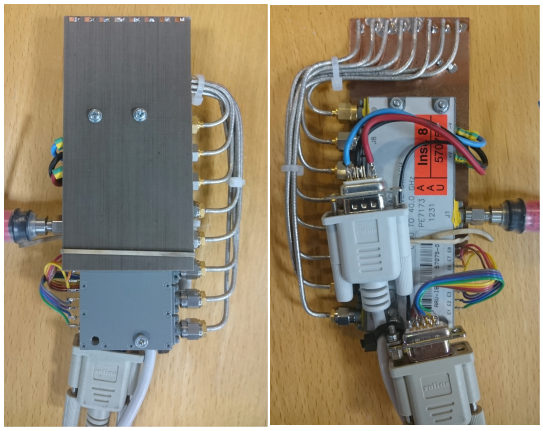

Fig. 1: Mock-up handset. Left: the front which was pointing towards the user during the measurements. Right: back of the mock-up with the switch and control connectors.

Further dimensions of the mock-up are given in Fig. 2. As explained in [37], the designed mock-up antenna array offers good efficiency, good S-parameters at the operating frequency, good impedance matching level and low mutual coupling. Each patch antenna element provides good radiation behavior, with a 5 dBi directive pattern towards the user direction. The radiation behavior for the constructed mock-up was validated in measurements. The added absorptive switch and cabling resulted in only minor impact on the performance of the patch elements when compared to the design presented in [37]. This is mainly due to the use of patches which will not excite strong surface currents as discussed in [38].

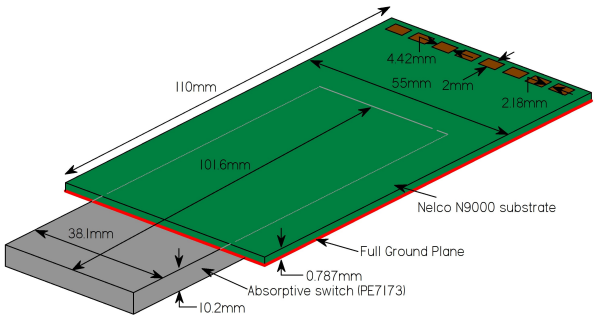


Fig. 2: Sketch of the mock-up handset including dimensions. Partly redrawn from [37].

### B. Tx antenna

A dual-polarized standard-gain horn antenna is utilized as the Tx antenna (A-INFO LB-SJ180400). The horn antenna covers 18 GHz to 40 GHz, with a 3 dB beamwidth $46.8°$ for the H-plane and $37.2°$ for the E-plane at 21.5 GHz. The Tx antenna gain is around 12 dBi at 21.5 GHz. The vertical and horizontal polarization of the used antenna are driven by Tx branch Tx1 and Tx2, respectively, as explained in the following.

### C. Channel sounder

The measurements were performed using a wideband MIMO channel sounder developed at Aalborg University. The channel sounder is based on the pseudo noise (PN) correlation principle; its fundamentals are described in [39]. The latest version, covering carrier frequencies up to 40 GHz, was used in [40]. The specific parameters of the system as used in the current work are presented in Fig. 3.

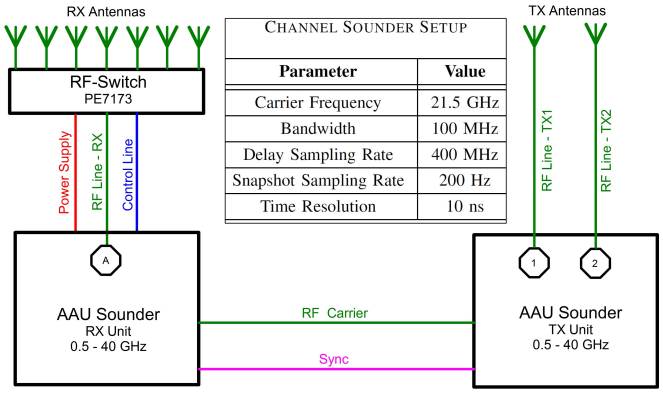


CHANNEL SOUNDER SETUP

| Parameter | Value |
|---|---|
| Carrier Frequency | 21.5 GHz |
| Bandwidth | 100 MHz |
| Delay Sampling Rate | 400 MHz |
| Snapshot Sampling Rate | 200 Hz |
| Time Resolution | 10 ns |

Fig. 3: Schematic and settings for the channel sounder setup. Note that the two Tx antennas shown are the two different polarization feeds of the same dual polarized horn antenna.

As explained in [39], the wideband channel sounder can support quasi-simultaneous measurements, via parallel branches at both the Tx and Rx, combined with fast switching.

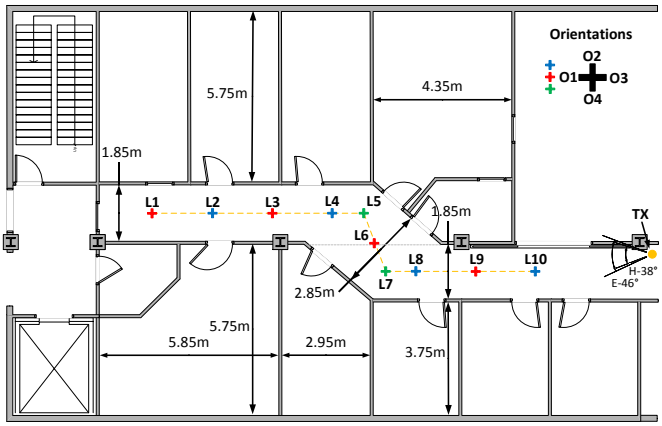


Fig. 4: Floor plan showing the locations for the measurements. In the top right corner a reference for the orientations (O) used at the different locations (L) is shown.

Fig. 5: Pictures of the corridor where the measurement was conducted. Left is seen the setup for measuring in free space. Right is seen a measurement including a user.

In the current measurement campaign, two Tx branches were recorded in parallel for each Rx, and this was repeated 7 times via a fast switch at the Rx. Note that only 7 Rx antenna elements of the mock-up array were utilized due to limitations of the practical setup (one antenna on the edge not used).

The total measurement time to record $2\times7$ complex channel impulse responses (CIRs) for all Tx and Rx branches is about 573 $\mu$s. The channel was measured at a rate of 200 Hz and a total of 50 snapshots of the channel were collected for each measurement.

### D. Measurement Scenarios

The measurement campaign was conducted in a typical indoor corridor scenario in a modern office building. The floor plan of the scenario is shown in Fig. 4 and pictures are shown in Fig. 5.

As indicated in Fig. 4, the Tx antenna was placed in the corridor at a height of 205 cm on a wooden pole, with the main beam pointing towards the Rx locations in the corridor, mimicking an indoor access point scenario. The Tx was kept in the same position throughout the entire measurement campaign.

Both line of sight (LOS) (i.e. locations L7 to L10) and non-line of sight (NLOS) (i.e. locations L1 to L6) scenarios were considered for the Rx, as shown in Fig. 4. The measurement locations were distributed following a reference line from left to right in Fig. 4. Most measurement locations were placed in the middle of the corridor except L5 and L7, which were placed closer to the walls.

At every location, four orientations (O) of the user with handset were considered, as shown in the top right corner of Fig. 4. O1 was orientated such that the user looked away from the Tx, and the other three orientations (O2-4) were obtained, with $90^o$ step in a clockwise way, as shown in Fig. 4. The different Rx locations and orientations were measured using different operation modes of the mock-up handset, as explained in the following.

### E. Operation modes

Two different operation modes were investigated, free space mode and user influence mode. As for the user influence mode, so-called 'data mode' was considered, where the user holds the DUT in both hands, as shown in Fig. 6.

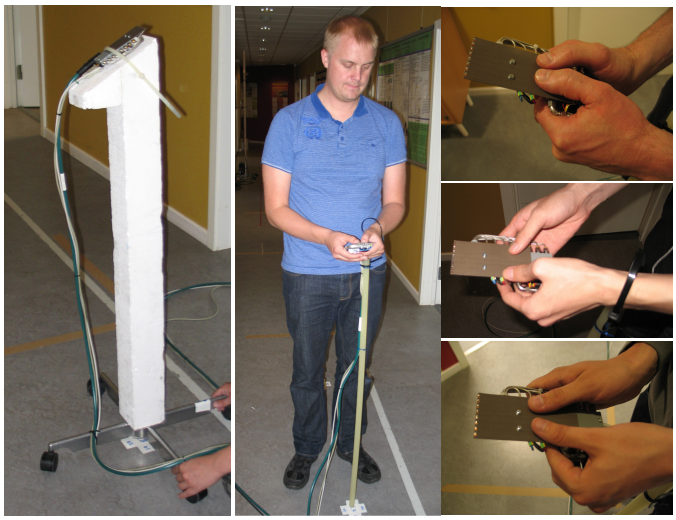

Fig. 6: The left picture shows the pedestal for measuring in the free space mode. The middle picture illustrates the positioning with a user. Note that the guide stick is centered at the same point as the free space pedestal. Right pictures show how different users holds the mock-up handset.

*1) Free Space Mode:* The free space mode represents the case where no user is present. This was realized by placing the mock-up on a column of expanded polystyrene (EPS - $\epsilon_r \approx 2.25$) with minimal influence on the fields. As shown in Fig. 6 (left), the mock-up was placed at the height of 120 cm and slanted $30^o$ with respect to the azimuth plane, similar to the height and angle as when held by a user.

The EPS column, with mock-up, was placed with its center at each measurement location and orientation, as explained above. During each measurement, the EPS column was moved in a circular manner without changing the orientation of the mock-up. The radius for the movement was roughly 5 cm,

which is equivalent to slightly more than 3.5 wavelengths at 21.5 GHz. The movement during the measurement allows for different realizations of the multipath channel. Note that measurement locations L5 and L7 were repeated 10 times for each orientation.

*2) User influence mode:* In the user influence mode, we intend to follow the same procedure as described in the free space mode. To achieve this, each user was instructed to move the handset in a circular fashion with the similar radius (i.e. 5 cm) as in the free space mode. To ensure a comparable height of the Rx, the user's wrist was guided by a stick of polyethylene (PE - $\epsilon_r \approx 2.25$), as illustrated in the middle of Fig. 6. Further, the elevation angle of the mock-up handset was aligned to 30° before the start of the measurement. However, due to the different styles of grip, as seen in the right photos in Fig. 6, variations between users might be present. This is intentional since this kind of variation must be expected for practical devices. The measured environment was kept largely static, except that the user holding the mockup was moving as instructed.

A total of 5 users were involved in the measurement campaign to allow for a study of the impact of different users. All 5 users were of similar height and body shape. At location L5 and L7, 10 repetitions of each measurement were conducted with user 1 and 2, and 3 repetitions for user 3, 4 and

## III. Measurement Results

A total of 504 measurements, including repetitions at some locations, was conducted and used for the presented results. The datasets contains the following parameters:

- 10 Locations (L1-10)
- 4 Orientations (O1-4)
- 6 Operation Modes (FS and U1-5)
- 2 Polarizations (Tx1 and Tx2)
- 7 Array elements (Rx1-7)

where L denotes location, O orientation, FS free-space and U denotes user. Tx1 and Tx2 denotes, respectively, the horizontal and vertical Tx polarization. Rx1-7 denotes the 7 elements/branches in the used linear array.

The current work focuses on the mean power gain defined as

$$P(t,r) = \frac{1}{NM} \sum_{n=1}^{N} \sum_{m=1}^{M} |h(t,r,n,m)|^2 \qquad (1)$$

where $h(t,r,n,m)$ is the complex impulse response at the $n$-th time-index, the $m$-th delay-index, where $t \in \{1,2\}$ is the Tx index, and $r \in \{1,\dots 7\}$ is the Rx branch index. Thus, $P(t,r)$ is the mean wideband power of the instantaneous channel between the $t$-th transmitter and $r$-th receiver antenna element. The number of channel snapshots in each measurement is $N = 50$ and $M = 500$ is the number of samples in delay.

Five studies are presented in the following sub-sections. The first is focusing on the mean power in free space conditions, then mean influence of the user is studied, followed by the differences in power due to the users, then the branch power ratios (BPRs) of the Rx array, and finally differences due to the Tx polarization.

### A. Free Space

In the following study, the presented total mean power is found as the mean power over all seven Rx elements. For the measurement locations including repetitions (L5 and L7) the expressed power is given as the mean power of the repetitions.

The resulting mean total power for the free space measurement is presented in Fig. 7 for all the measurement locations. As expected the received power decreases with distance, given that the lower the location number, the further away from Tx, as seen in Fig. 4. This is emphasised by the added interpolation between measurement locations in Fig. 7. In strict sense data is only available for the individual measurement locations and the added curves must therefore only been seen as an estimation of the expected power between measurement locations.

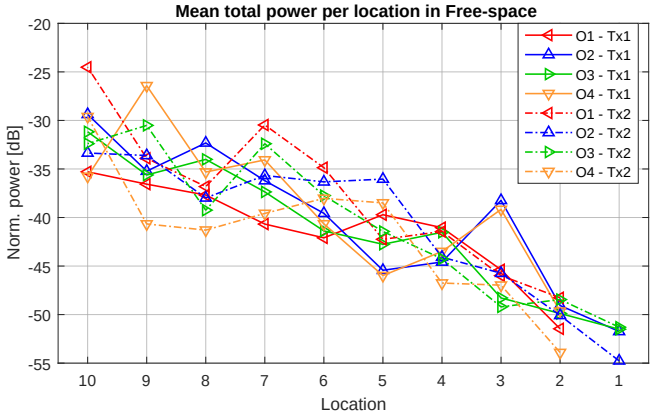


Fig. 7: Mean total power in the free space scenario for the four orientations (O) shown for all the locations and both polarizations (Tx1 and Tx2). The points indicate measured values, while the connecting lines are only for visualization

The mean power variation in free space due to the change of orientation is up to 10 dB in the same polarization. The variation between polarizations, even for the same orientations, is up to 14 dB. The power difference between polarizations tends to diminish with distance to the Tx except for L3. Here the vertical polarization shows significantly higher power. This could be a result of favorable geometry for this specific location and orientation of the antenna.

For especially O4 - Tx1, in Fig. 7, it seems like L10 has much lower power than L9. This is explained by the proximity of L10 to the Tx and the height of the Tx and Rx. In this scenario the Rx is below the main lobe of the Tx antenna and therefore not illuminated to the same degrees as it is the case for Rx in L9.

Note that some values in Fig. 7 (and later plots) are missing, since they were discarded due to a too low quality of the measurements (typically a low dynamic range).

### B. Mean Influence of the User on Power

The mean influence of the user is computed as the mean of the total power obtained with the different users and normalized with the total power gain obtained in free space for

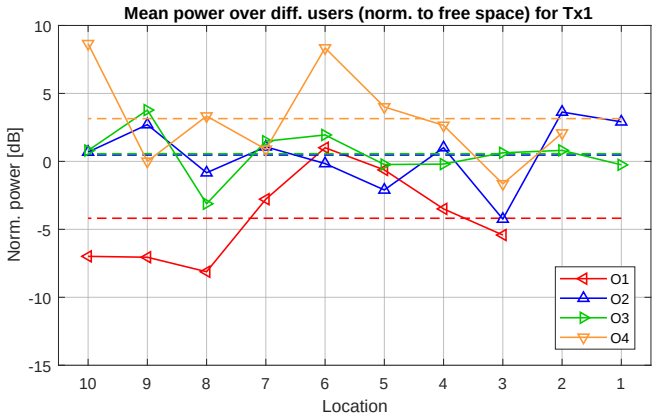


Fig. 8: Total power gain for Tx1, averaged over the five users and normalized to the similar channel in free space with same location and orientation. The points indicate measured values, while the connecting solid lines are only for visualization. The dashed lines indicate mean values.

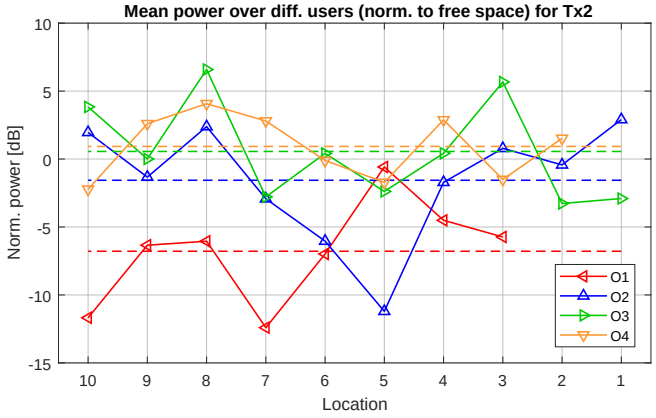


Fig. 9: Total power gain for Tx2, plotted in the same manner as Fig. 8.

the same location and orientation combination. Fig. 8 shows the results for Tx1, while Fig. 9 shows similar reults for Tx2.

An interesting finding is that the power in many cases is higher in the measurements with a user than for free space measurements, corresponding to positive values in Fig. 8 and Fig. 9. This is especially the case for O4 - Tx1. For L9 the power is the same in the two scenarios but from L8 to L2 the power is up to 8 dB higher when the user is present.

This is explained by seeing the user as an added scatterer in the scenario. The user will reflect some power towards the Rx and in the case of O4, this is most pronounced. The linear patch array elements in the mock-up handset have maximum directivity perpendicular to its plane and therefore focused towards the user when held in front. In the case of O4, the user is orientated towards the west corridor wall, as seen in Fig. 4. This orientation will give the least blocking and the user will reflect some of the power back towards the direction of maximum antenna directivity, overall improving the gain. A similar phenomena was seen in the measurements presented in [36]. In this study the user effect on the handset antenna was studied in the anechoic chamber.

From both Fig. 8 and Fig. 9, it is clear how the users introduce a significantly higher loss for O1 at the locations L10 to L7, which correspond to the LOS part of the measurement scenario. O1 is the orientation where the user has its back to the Tx and therefore imposes the largest blocking for the Rx. For Tx2, a large loss is also seen for O2 at L5 and L6. In this location, O2 corresponds to having the user in between the reflected path from the Tx and the Rx. In L4 and L3 O1 is again the orientation with the highest blocking effect.

As evident from the two figures, the user impact is highly dependent on both orientation and location, with both positive up to about 9 dB for Tx1-L10-O4 and negative down to about $-12$ dB for Tx2-L10-O4. These cases are observed for the shortest distance where the LOS will be dominant compared to any multipath.

### C. Power Variation with User

The user influence on the power gain is likely to depend on the individual user, due to different ways of holding the mockup handset, different size, *etc.* This is analyzed in the following.

As described in Sec. II-E, measurements are obtained with five users for all locations and orientations. Fig. 10 – 11 shows the mean power for each individual user, normalized to the mean value of all users for each location-orientation case. The normalization to the mean power is conducted in order to illustrate the variation in mean power between users.

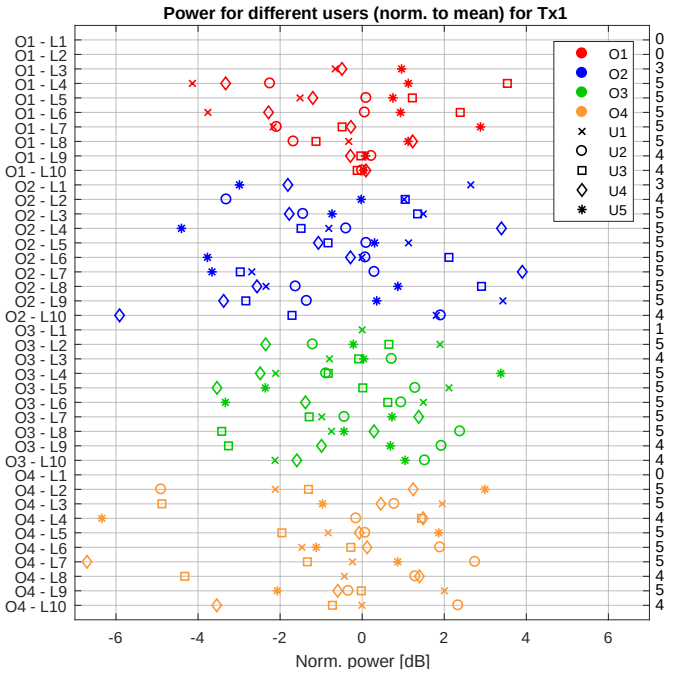


Fig. 10: The mean power for Tx1 for different users sorted by orientation, as seen in the left vertical axis. The data points are normalized to the mean power of the users. Only one measurement repetition per user is included. The orientation (O) has been indicated by colors and the five different users (U) by different symbols. The number of successful measurements for each orientation-location combination in shown on the right vertical axis.

In Fig. 10 and Fig. 11 the data is sorted according to the orientation (O) as shown in the left vertical axis. For

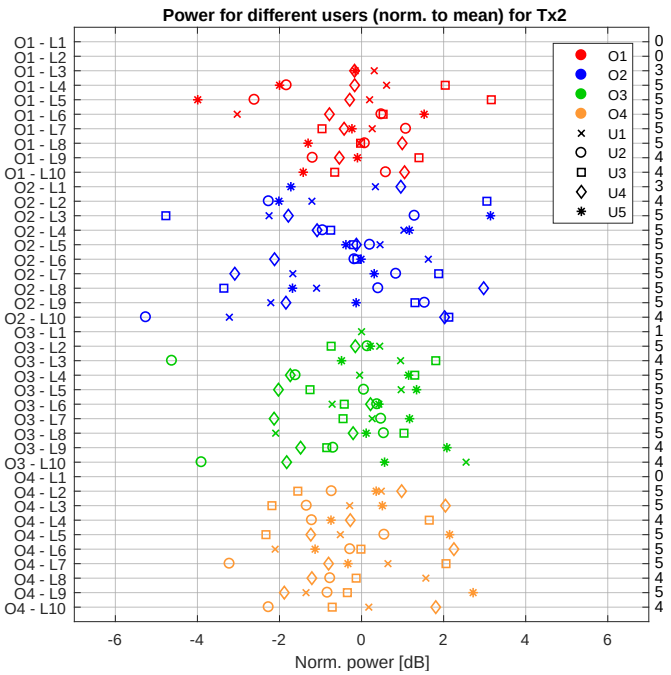


Fig. 11: The mean power for Tx2, plotted in the same manner as Fig. 10.

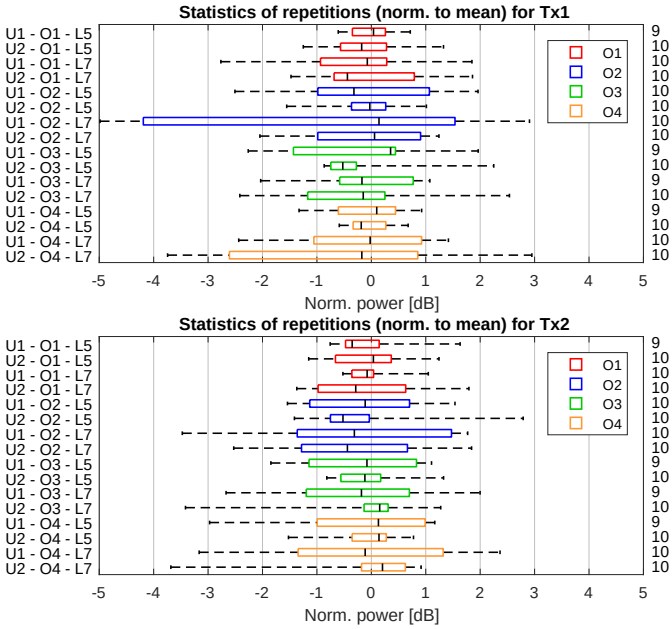


Fig. 12: The power variation of different repetitions, normalized to the mean of the repetitions. Plotted for user (U) 1 and 2 at location (L) 5 and 7 for all orientations (O) as shown on the left vertical axis. The right vertical axis indicates the number of data points used for the box-plot. The maximum variation of the data is shown using the whiskers while the box indicates the lower 25- and upper 75-percentile limits. The black marker in the boxes indicates the median.

each combination the results from the measurements with each of the five users are shown with symbols, according to the normalized power. Even though five users were used for all orientations, some measurements were discarded, as mentioned previously, and thus no points were shown (e.g. for O1-L1). The number of users per orientation-location combination is indicated by the right vertical axis. Also note that only a single repetition is shown for each user, i.e., no repeated values are included.

From Tx1, in Fig. 10, it can be noted that almost all the values are in the range $\pm 6$ dB with the majority within $\pm 4$ dB. For Tx2, in Fig. 11, the values are slightly less spread with the majority of values within $\pm 2$ dB. In both cases no general pattern is evident between the different users when sorted according to the orientation. It is noted that sorting the data according to location neither resulted in any general pattern.

To investigate the repeatability of the measurements, the repeated measurement at location L5 and L7 with user U1 and U2 have been used. These user-location combinations are used as they are numerous enough for a box-plot, showing the statistical properties.

The repetition measurement was conducted in a sequential manner to limit the impact of other factors rather than the slight change in grip-styles among different users between measurements.

From Fig. 12 it can be seen that the variation of the mean power was up to 5 dB. The majority of the measurement repetitions showed a variation of less than 1 dB. An interesting observation is the larger variation between repetitions of the same measurement using O1 and O2. This could indicate that the specific location-orientation combination is especially susceptible to slight changes of the grip-style.

### D. Rx Element Power Ratio

An array of antenna elements may potentially be used for either diversity or to form beams, which is generally envisioned as very important for utilizing millimetre- and centimetre-waves in cellular systems.

In practice, the antenna elements can not be expected to be identical and in addition, the element properties may be changed in the presence of the user and other parts of the surroundings. The effectiveness of diversity schemes depends highly on the Rx branches having approximately equal power. Similarly, for beamforming to work any differences in the element properties may have to be known, possibly from estimation.

To illustrate the variation between the received power of the 7 Rx elements, they have been plotted for location L7 and L5 in, respectively, LOS and NLOS. The plots for the two locations are shown in Fig. 13 and Fig. 14, where the measured average power for the different Rx elements are shown both in free space and with a user.

Fig. 13 and Fig. 14 clearly indicate that mean power is not uniform among the elements. The element power for the used array shows variations up to 13 dB in the free-space scenario and 7 dB including a user. The largest variation between elements is seen in free-space (FS) at L7 for O2 in the Tx1 polarization between element Rx1 and Rx7 as seen in Fig. 13. For the user scenario (U) the largest variation is seen at L5 for O3 in the Tx1 polarization between element Rx1 and Rx5 as seen in Fig. 14.

The most pronounced user influence is seen at O1 in Fig. 13 and at O2 for TX2 as seen in Fig. 14. When the blocking

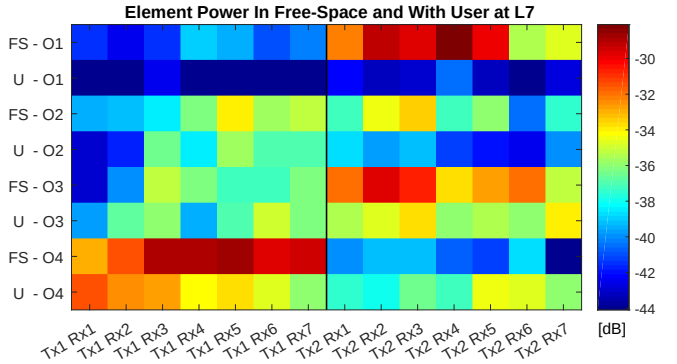


Fig. 13: Plot of the variation in mean power for the seven elements (Rx) in free space (FS) and with a user (U) for the different orientations (O) and the two polarizations (Tx1/Tx2) for L7.

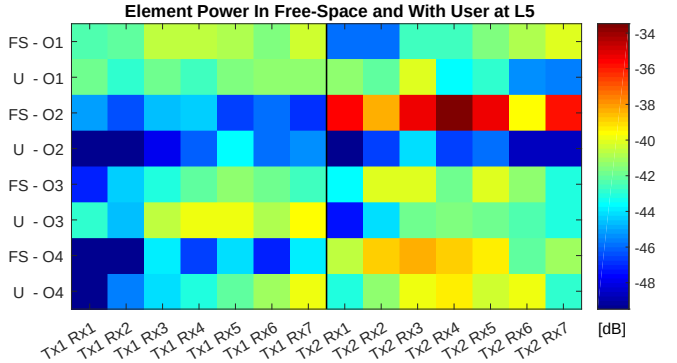


Fig. 14: Plot of the variation in mean power for the seven elements (Rx) in free space (FS) and with a user (U) for the different orientations (O) and the two polarizations (Tx1/Tx2) for L5.

occurs, it can be seen that all the elements are affected. The blocking causes more than 10 dB drops in power for some elements, while some elements show more than 10 dB increase when the user is present. Note that this improvement of the performance of the array is only possible if the users' hand is not in the vicinity of the antenna, hence affecting the radiation performance.

A simple and first approach to statistically evaluate the challenges in using array techniques for user held equipment is to study the branch power ratio (BPR) between the antenna elements. For simplicity, only the maximum BPR (mBPR) is studied here. Denoting the average channel gain by $P(Tx,Rx)$, as in Eq. 1, the mBPR is defined as:

$$\beta(t) = \frac{\max\limits_{r} P(t,r)}{\min\limits_{r} P(t,r)} \tag{2}$$

where $t \in \{1,2\}$ is the Tx index, and $r \in \{1,\ldots 7\}$ is the Rx branch index. The mBPR will be determined by a combination of the antenna properties and the propagation in the channel.

To maximize the amount of measurement data used for calculating the mBPR, both data from the free-space and user scenario together with any repetitions have been used. Due to this large dataset, the individual points have not been indicated with user symbols as inFig. 10 and Fig. 11 but only simple points as seen in Fig. 15. The data presented in Fig. 15 shows the complete data set but can be difficult to read. Due to this, box-plots have been used to describe the statistical properties, as seen in Fig. 16. Special attention should be given to the number of used data points for each orientation-location combination. This is indicated along the right vertical axis in the figures allow the reader to judge the underlying data, especially for the orientation-location combinations with few data points.

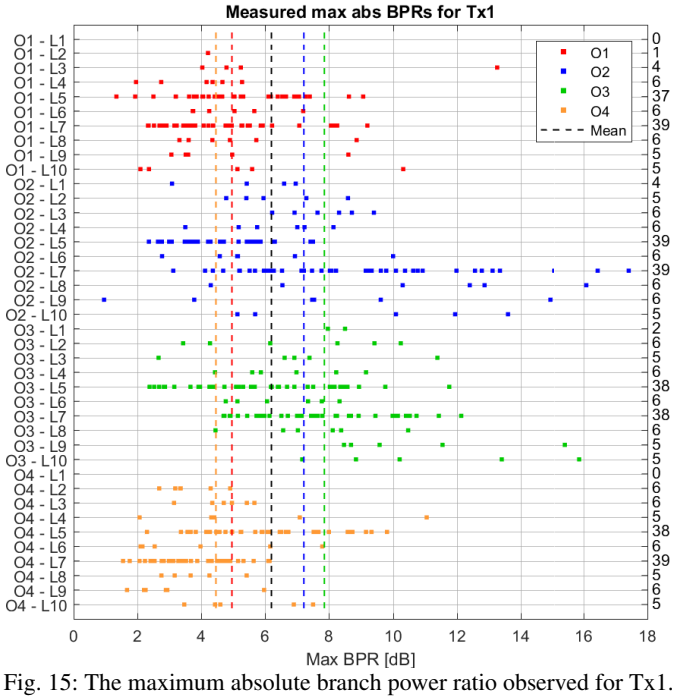


Fig. 15: The maximum absolute branch power ratio observed for Tx1. Data points are shown for both free space and user cases, including repetitions, for the given orientation-location combination shown on the left vertical axis. The right vertical axis indicates the number of data points. The used colors corresponds to the four orientations (O) which mean mBPR is indicated with a dashed line. The mean for all data points is marked by a black dashed line.

Fig. 16 and Fig. 17 shows that the majority of the mBPR values are in the range 2–10 dB. The figures also show that large variations in mBPR are present, even for the different measurements obtained with the same location and orientation combination. The highest mBPR, for both Tx1 and Tx2, is found for O3 and O4 at L7-10. This corresponds to the locations (L) closest to the transmitter (LOS) and the user facing the north wall and towards the transmitter, as seen in Fig. 4. Interestingly, it seems that the LOS locations experience more severe power variations. The largest difference in mean values, as seen when comparing Fig. 16 and Fig. 17, is found for Tx1. Hence, Tx1 corresponding to the vertical polarization, is more sensitive to the orientation than Tx2 for the chosen propagation scenario.

### *E. Tx Polarization Influence on Rx Power*

From the previous studies, it has become evident that there is a measurable difference between the vertical and horizontal polarization, denoted by Tx1 and Tx2, respectively. Even if a system transmits in only one polarization, some of the power in many cases will be coupled in the channel to the other polarization. While in practice most handset antennas will

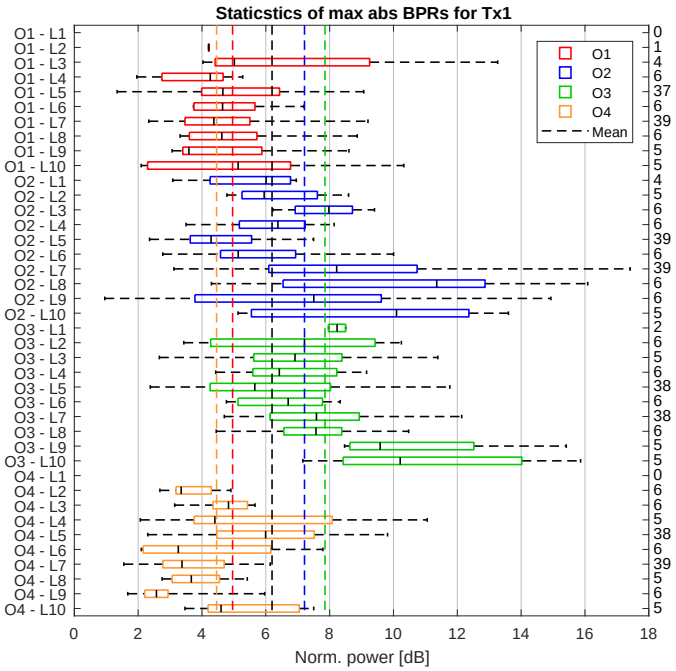


Fig. 16: The statistics of the maximum absolute branch power ratio observed for Tx1 plotted as box-plots following the same practice as Fig. 15. The maximum variation of the data is shown using the whiskers while the box indicates the lower 25- and upper 75-percentile limits. The black marker in the boxes indicates the median for the given orientation-location combination.

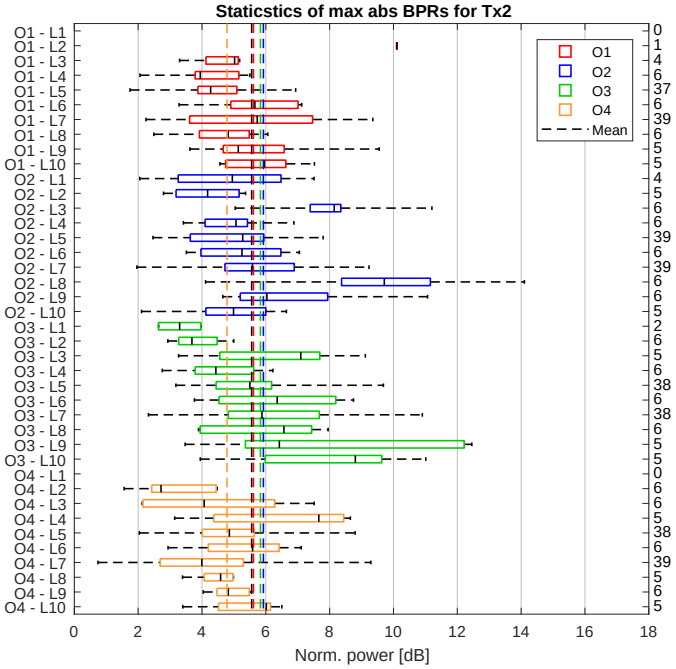


Fig. 17: The statistics of the maximum absolute branch power ratio observed for Tx2, plotted in the same manner as Fig. 16.

receive in both polarizations, depending on the design and usage, especially the orientation of the device, it is complicated to predict which is preferable, if any. This is jointly determined by the antenna/handset properties, the random influence of the user, as well as the channel.

The polarization power ratio (PPR) $\gamma$ is defined as the ratio of the average power received when transmitting in the two different polarizations as:

$$\gamma = \frac{\sum_{r_1=1}^{R} P(t=1,r_1)}{\sum_{r_2=1}^{R} P(t=2,r_2)} \tag{3}$$

where $R = 7$ is the total number of Rx antennas and $P(\cdot)$ is defined as previously in connection with Eq. 1.

With the current measurements, the channels for Tx1 and Tx2 are measured at the same time physically so it is possible to evaluate the PPR in the exact same conditions with the user location and orientation. Like for the BPR study in Sec. III-D, the results for both free space, users and all repetitions are included to use as large a data set as possible. The resulting PPR plot is therefore also presented in Fig. 18 as a box-plot. Each orientation-location combination is a line in the box-plots and the mean values for the four orientations are indicated by dashed lines.

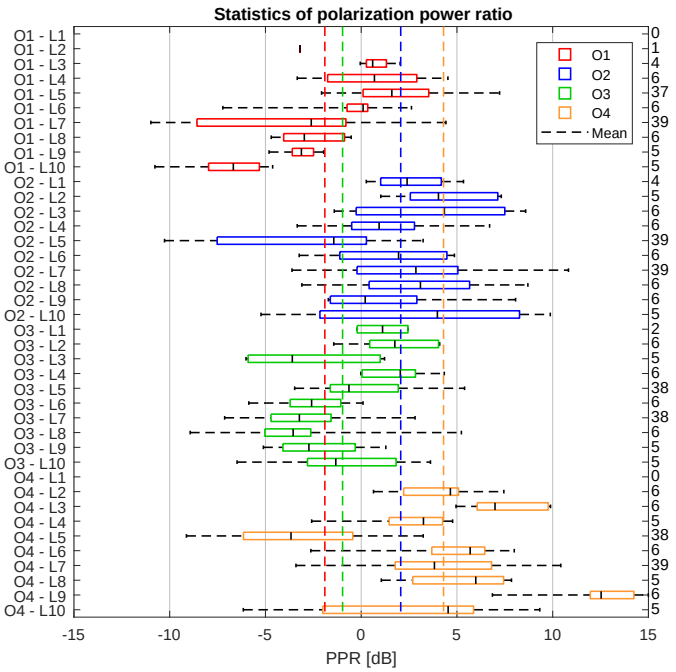


Fig. 18: The statistics of the polarization power ratio for all the measured scenarios and users, including free space plotted in the same manner as Fig. 16.

Fig. 18 shows that most measurements have a PPR within a range of $\pm 10$ dB, with large variations among the different measurements for the same orientation-location combinations. Thus, the polarization state is highly sensitive to the exact channel conditions. Further, Fig. 18 shows that there is a tendency of a lower PPR for O1 when getting closer to the Tx (higher number), probably because of a more pure polarization in the channel. A similar tendency is found for O3, while it is more mixed for O2 and O4.

## IV. Discussion

Based on the results presented in the previous section some discussions and speculations can be made on the impact of the findings. This is presented in the following section.

In Sec. III-A the measurements showed, as expected, that an increasing distance from Tx to Rx results in an increasing path-loss. The path-loss at especially the NLOS locations are high. However, the signal is still reaching locations deep in NLOS, likely mainly via reflections. The measurements presented in Sec. III-B shows that the user blocks the LOS component in the LOS scenario and the expected dominant path in the NLOS scenario. The large impact on received power caused by the user blocking needs to be considered in future system designs.

Sec. III-C describes variation in the received mean power of up to almost 7 dB among the 5 different users, as seen in Fig. 10. It is noted that the variation in mean power for repetitions of the measurement was up to 5 dB, as seen in Fig. 12. As expected, the measurements with a user generally had higher losses when compared to a free-space measurement. However, in some cases, a gain was found. This can be explained by the user acting as an added scatterer, which in some specific scenarios can improve the link. The data obtained with the different users showed no apparent pattern, even when measured at the same orientation-location. This indicates that the user influence can be seen as a random factor.

The high path-loss together with the possible added losses due to the user has to be overcome to enable a future millimetre-wave system. One method is to apply beamforming facilitating a high gain. As shown in Sec. III-D, the measurements showed large variations in BPR of up to almost 18 dB, as seen in Fig. 15 and Fig. 16. Overall, these variations can be caused by fading over the array due to multipath in the channel, by the influence of the user, or a combination. Beamforming would be effective in the case of multipath, but if the power variations are caused by other mechanisms, such as absorption in the users' fingers or changes in the element radiation pattern, implementing effective beamforming could be difficult.

The investigation of the two polarizations described in Sec. III-E showed a PPR of up to 15 dB, indicating that there is a large gain to be obtained if future systems utilize both polarizations at the access point. However, it is also important to realize that the PPR changes both due to the environment and the user. The handset will, in most cases, transmit or receive in a mixture of both polarizations and the user will likely also change the orientation of the handset. Therefore, the system needs to adapt to the polarization coupling in the channel.

## V. Conclusion

Based on $21.5\,\mathrm{GHz}$ channel measurements performed in an indoor scenario the impact of the user holding the receiving handset antenna is studied.

The measurement campaign includes both free space conditions and users. Five different users have been measured in an indoor corridor scenario at ten different locations and with four different orientations. The users hold the mock-up handset in data mode.

The mean influence of the user's on the power vary significantly depending on the location and orientation of the user, with a loss of more than 12 dB in some cases. The mean power loss is among the different locations is less than about 7 dB, depending on the orientation.

The measurements also indicate that the user can also help the link by acting as a scatterer, given that the user is not in a direct blocking position. This gain from the user is up to about 4 dB for the most favorable orientation. However, the effect is less than $2\,\mathrm{dB}$ for the other orientations.

Among the five users, considerable variation in the mean power was also found. The variation was typically within $\pm 4$ dB.

The mock-up handset was equipped with a 7-element array, potentially useful for e.g. beamforming or diversity. For such applications, differences in average power among the elements may be critical. Therefore, the maximum branch power ratio (mBPR) was investigated for the measured data. Large variations were found, with absolute mBPR values typically in the range 2–10 dB, mostly depending on the individual user or measurement.

With the chosen handset mock-up the difference in received power when transmitting in either vertical or horizontal polarization depends highly on the exact measurement condition, with ratios of mean power in the range $\pm 10$ dB. Thus, both Tx polarizations are needed in practice for best power transfer.

## Acknowledgment

The authors would like to thank Kim Olesen, Anders Karstensen, Yilin Ji and Stanislav Zhekov for valuable assistance with the measurements. Further the authors would like to thank Ming Shen for providing the mock-up antenna used for the measurement.

## References

[1] P. Demestichas, A. Georgakopoulos, D. Karvounas, K. Tsagkaris, V. Stavroulaki, J. Lu, C. Xiong, and J. Yao, "5g on the horizon: Key challenges for the radio-access network," *Vehicular Technology Magazine, IEEE*, vol. 8, no. 3, pp. 47–53, Sept 2013.

[2] Q. Li, H. Niu, A. Papathanassiou, and G. Wu, "5g network capacity: Key elements and technologies," *Vehicular Technology Magazine, IEEE*, vol. 9, no. 1, pp. 71–78, March 2014.

[3] L. Wei, R. Q. Hu, Y. Qian, and G. Wu, "Key elements to enable millimeter wave communications for 5g wireless systems," *IEEE Wireless Communications*, vol. 21, no. 6, pp. 136–143, December 2014.

[4] Ofcom, "Spectrum above 6 ghz for future mobile communications," Ofcom UK, Riverside House, 2a Southwark Bridge Road, London, Consultation Report, January 2015.

[5] S. Methley, W. Webb, S. Walker, and J. Parker, "Study on the suitability of potential candidate frequency bands above 6ghz for future 5g mobile broadband systems," Quotient Associates Limited, Compass House, Vision Park, Chivers Way Histon, Cambridge, CB24 9AD, UK, Technical Report, March 2015.

[6] T. Rappaport, S. Sun, R. Mayzus, H. Zhao, Y. Azar, K. Wang, G. Wong, J. Schulz, M. Samimi, and F. Gutierrez, "Millimeter wave mobile communications for 5g cellular: It will work!" *Access, IEEE*, vol. 1, pp. 335–349, 2013.

[7] S. Rangan, T. Rappaport, and E. Erkip, "Millimeter-wave cellular wireless networks: Potentials and challenges," *Proceedings of the IEEE*, vol. 102, no. 3, pp. 366–385, March 2014.

[8] W. Hong, K. H. Baek, Y. Lee, Y. Kim, and S. T. Ko, "Study and prototyping of practically large-scale mmwave antenna systems for 5g cellular devices," *IEEE Communications Magazine*, vol. 52, no. 9, pp. 63–69, September 2014.

[9] W. Roh, J.-Y. Seol, J. Park, B. Lee, J. Lee, Y. Kim, J. Cho, K. Cheun, and F. Aryanfar, "Millimeter-wave beamforming as an enabling technology for 5g cellular communications: theoretical feasibility and prototype results," *Communications Magazine, IEEE*, vol. 52, no. 2, pp. 106–113, February 2014.

[10] S. Han, C. l. I, Z. Xu, and C. Rowell, "Large-scale antenna systems with hybrid analog and digital beamforming for millimeter wave 5g," *IEEE Communications Magazine*, vol. 53, no. 1, pp. 186–194, January 2015.

[11] T. Rappaport, F. Gutierrez, E. Ben-Dor, J. Murdock, Y. Qiao, and J. Tamir, "Broadband millimeter-wave propagation measurements and models using adaptive-beam antennas for outdoor urban cellular communications," *Antennas and Propagation, IEEE Transactions on*, vol. 61, no. 4, pp. 1850–1859, April 2013.

[12] H. Xu, V. Kukshya, and T. S. Rappaport, "Spatial and temporal characteristics of 60-ghz indoor channels," *IEEE Journal on Selected Areas in Communications*, vol. 20, no. 3, pp. 620–630, Apr 2002.

[13] N. Moraitis and P. Constantinou, "Indoor channel measurements and characterization at 60 ghz for wireless local area network applications," *IEEE Transactions on Antennas and Propagation*, vol. 52, no. 12, pp. 3180–3189, Dec 2004.

[14] P. F. M. Smulders, "Statistical characterization of 60-ghz indoor radio channels," *IEEE Transactions on Antennas and Propagation*, vol. 57, no. 10, pp. 2820–2829, Oct 2009.

[15] S. Geng, J. Kivinen, X. Zhao, and P. Vainikainen, "Millimeter-wave propagation channel characterization for short-range wireless communications," *IEEE Transactions on Vehicular Technology*, vol. 58, no. 1, pp. 3–13, Jan 2009.

[16] S. Salous, S. M. Feeney, X. Raimundo, and A. A. Cheema, "Wideband mimo channel sounder for radio measurements in the 60 ghz band," *IEEE Transactions on Wireless Communications*, vol. 15, no. 4, pp. 2825–2832, April 2016.

[17] A. Sulyman, A. Nassar, M. Samimi, G. Maccartney, T. Rappaport, and A. Alsanie, "Radio propagation path loss models for 5g cellular networks in the 28 ghz and 38 ghz millimeter-wave bands," *Communications Magazine, IEEE*, vol. 52, no. 9, pp. 78–86, September 2014.

[18] R. J. C. Bultitude, R. F. Hahn, and R. J. Davies, "Propagation considerations for the design of an indoor broad-band communications system at ehf," *IEEE Transactions on Vehicular Technology*, vol. 47, no. 1, pp. 235–245, Feb 1998.

[19] G. A. Kalivas, M. El-Tanany, and S. Mahmoud, "Millimeter-wave channel measurements with space diversity for indoor wireless communications," *IEEE Transactions on Vehicular Technology*, vol. 44, no. 3, pp. 494–505, Aug 1995.

[20] H. Xu, T. S. Rappaport, R. J. Boyle, and J. H. Schaffner, "Measurements and models for 38-ghz point-to-multipoint radiowave propagation," *IEEE Journal on Selected Areas in Communications*, vol. 18, no. 3, pp. 310–321, March 2000.

[21] W. Fan, I. C. Llorente, J. Ødum Nielsen, K. Olesen, and G. F. Pedersen, "Measured wideband characteristics of indoor channels at centimetric and millimetric bands," *EURASIP Journal on Wireless Communications and Networking*, vol. 2016, no. 1 -Special issue on Radio Channel models for higher frequency bands, pp. 1–13, 2016.

[22] G. R. Maccartney, T. S. Rappaport, S. Sun, and S. Deng, "Indoor office wideband millimeter-wave propagation measurements and channel models at 28 and 73 ghz for ultra-dense 5g wireless networks," *IEEE Access*, vol. 3, pp. 2388–2424, 2015.

[23] M. D. Kim, J. Liang, H. K. Kwon, and J. Lee, "Path loss measurement at indoor commercial areas using 28ghz channel sounding system," in *2015 17th International Conference on Advanced Communication Technology (ICACT)*, July 2015, pp. 535–538.

[24] P. B. Papazian, K. A. Remley, C. Gentile, and N. Golmie, "Radio channel sounders for modeling mobile communications at 28 ghz, 60 ghz and 83 ghz," in *Millimeter Waves (GSMM), 2015 Global Symposium On*, May 2015, pp. 1–3.

[25] S. Hur, Y.-J. Cho, J. Lee, N.-G. Kang, J. Park, and H. Benn, "Synchronous channel sounder using horn antenna and indoor measurements on 28 ghz," in *Communications and Networking (BlackSeaCom), 2014 IEEE International Black Sea Conference on*, May 2014, pp. 83–87.

[26] S. Salous and Y. Gao, "Wideband measurements in indoor and outdoor environments in the 30 ghz and 60 ghz bands," in *2016 10th European Conference on Antennas and Propagation (EuCAP)*, April 2016, pp. 1–3.

[27] S. Collonge, G. Zaharia, and G. E. Zein, "Influence of the human activity on wide-band characteristics of the 60 ghz indoor radio channel," *IEEE Transactions on Wireless Communications*, vol. 3, no. 6, pp. 2396–2406, Nov 2004.

[28] S. Obayashi and J. Zander, "A body-shadowing model for indoor radio communication environments," *IEEE Transactions on Antennas and Propagation*, vol. 46, no. 6, pp. 920–927, Jun 1998.

[29] K. Saito, T. Imai, and Y. Okumura, "Fading characteristics in the 26ghz band indoor quasi-static environment," in *Electromagnetics (iWEM), 2014 IEEE International Workshop on*, Aug 2014, pp. 135–136.

[30] J. Helander, K. Zhao, Z. Ying, and D. Sjöberg, "Performance analysis of millimeter-wave phased array antennas in cellular handsets," *IEEE Antennas and Wireless Propagation Letters*, vol. 15, pp. 504–507, 2016.

[31] K. Zhao, J. Helander, D. Sjoberg, S. He, T. Bolin, and Z. Ying, "User body effect on phased array in user equipment for 5g mm wave communication system," *IEEE Antennas and Wireless Propagation Letters*, vol. PP, no. 99, pp. 1–1, 2016.

[32] J. Toftgard, S. N. Hornsleth, and J. B. Andersen, "Effects on portable antennas of the presence of a person," *IEEE Transactions on Antennas and Propagation*, vol. 41, no. 6, pp. 739–746, Jun 1993.

[33] G. F. Pedersen and J. O. Nielsen, "Radiation pattern measurements of mobile phones next to different head phantoms," in *Vehicular Technology Conference, 2002. Proceedings. VTC 2002-Fall. 2002 IEEE 56th*, vol. 4, 2002, pp. 2465–2469 vol.4.

[34] G. F. Pedersen, K. Olesen, and S. L. Larsen, "Bodyloss for handheld phones," in *Vehicular Technology Conference, 1999 IEEE 49th*, vol. 2, Jul 1999, pp. 1580–1584 vol.2.

[35] J. B. Andersen, J. Ø. Nielsen, and G. F. Pedersen, "Absorption related to hand-held devices in data mode," *IEEE Transactions on Electromagnetic Compatibility*, vol. 58, no. 1, pp. 47–53, Feb 2016.

[36] I. Syrytsin, S. Zhang, G. Pedersen, K. Zhao, T. Bolin, and Z. Ying, "Statistical investigation of the user effects on mobile terminal antennas for 5g applications," *IEEE Transactions on Antennas and Propagation*, vol. Pre Press, 2017, "TO APPEAR".

[37] N. Ojaroudiparchin, M. Shen, S. Zhang, and G. Pedersen, "A switchable 3d-coverage phased array antenna package for 5g mobile terminals," *IEEE Antennas and Wireless Propagation Letters*, vol. PP, no. 99, pp. 1–1, 2016.

[38] S. Zhang, X. Chen, I. Syrytsin, and G. F. Pedersen, "A planar switchable 3d-coverage phased array antenna and its user effects for 28 ghz mobile terminal applications," *IEEE Transactions on Antennas and Propagation*, vol. PP, no. 99, pp. 1–1, 2017.

[39] J. Ø. Nielsen, J. B. Andersen, P. C. F. Eggers, G. F. Pedersen, K. Olesen, E. H. Sørensen, and H. Suda, "Measurements of indoor 16x32 wideband mimo channels at 5.8 ghz," in *Proceedings of the 2004 International Symposium on Spread Spectrum Techniques and Applications*, May 2004.

[40] J. Ø. Nielsen and G. F. Pedersen, "Dual-polarized indoor propagation at 26 ghz," in *2016 IEEE 27th International Symposium on Personal, Indoor and Mobile Radio Communications*, September 2016.

**Johannes Hejselbaek** received his Bachelor degree in Electronic Engineering with a specialization in communication systems in 2013 and a Master degree in Wireless Communication Systems in 2015, both from Aalborg University. He is currently a PhD Fellow at the department of antennas and propagation at Aalborg University. The focus of his work is on channel characterization and electromagnetic modeling in the cm/mm-wave domain.

**Jesper Ødum Nielsen** received his Master degree in electronics engineering in 1994 and a PhD degree in 1997, both from Aalborg University, Denmark. He is currently employed at Department of Electronic Systems at Aalborg University where main areas of interests are experimental investigation of the mobile radio channel and the influence mobile device users have on the channel. He has been involved in MIMO channel sounding and modeling, as well as measurements using live GSM and LTE networks. In addition he has been working with radio performance evaluation, including over the air testing of active wireless devices.

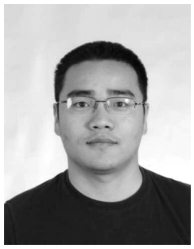

**Wei Fan** received his Bachelor of Engineering degree from Harbin Institute of technology, China in 2009, Master's double degree with highest honours from Politecnico di Torino, Italy and Grenoble Institute of Technology, France in 2011, and Ph.D. degree from Aalborg University, Denmark in 2014. From February 2011 to August 2011, he was with Intel Mobile Communications, Denmark as a research intern. He conducted a three-month internship at Anite telecoms oy, Finland in 2014. His main areas of research are over the air testing of MIMO terminals, radio channel modelling and virtual drive testing.

**Gert F. Pedersen** received the B.Sc. E. E. degree, with honour, in electrical engineering from College of Technology in Dublin, Ireland in 1991, and the M.Sc. E. E. degree and Ph.D. from Aalborg University in 1993 and 2003. He has been with Aalborg University since 1993 where he is a full Professor heading the Antenna, Propagation and Networking LAB with 36 researcher. Further he is also the head of the doctoral school on wireless communication with some 100 phd students enrolled. His research has focused on radio communication for mobile terminals especially small Antennas, Diversity systems, Propagation and Biological effects and he has published more than 175 peer reviewed papers and holds 28 patents. He has also worked as consultant for developments of more than 100 antennas for mobile terminals including the first internal antenna for mobile phones in 1994 with lowest SAR, first internal triple-band antenna in 1998 with low SAR and high TRP and TIS, and lately various multi antenna systems rated as the most efficient on the market. He has worked most of the time with joint university and industry projects and have received more than 12 M$ in direct research funding. Latest he is the project leader of the SAFE project with a total budget of 8 M$ investigating tunable front end including tunable antennas for the future multiband mobile phones. He has been one of the pioneers in establishing Over-The-Air (OTA) measurement systems. The measurement technique is now well established for mobile terminals with single antennas and he was chairing the various COST groups (swg2.2 of COST 259, 273, 2100 and ICT1004) with liaison to 3GPP for over-the air test of MIMO terminals. Presently he is deeply involved in MIMO OTA measurement.